J Clin Periodontol 2007; 34: 172–181 doi: 10.1111/j.1600-051X.2006.01014.x

Journal of Clinical Periodontology

Influence of controlled immediate loading and implant design on peri-implant bone formation

Katleen Vandamme[1], Ignace Naert[1], Liesbet Geris[2], Jozef Vander Sloten[2], Robert Puers[3] and Joke Duyck[1]

[1]Department of Prosthetic Dentistry/BIOMAT Research Group, School of Dentistry, Oral Pathology and Maxillofacial Surgery, Faculty of Medicine, K.U.Leuven, Leuven, Belgium; [2]Division of Biomechanics and Engineering Design, K.U.Leuven, Leuven, Belgium; [3]Department of Electrical Engineering–ESAT-MICAS, K.U.Leuven, Kasteelpark Arenberg, Leuven, Belgium

Vandamme K, Naert I, Geris L, Vander Sloten J, Puers R, Duyck J. Influence of controlled immediate loading and implant design on peri-implant bone formation. J Clin Periodontol 2007; 34: 172–181. doi: 10.1111/j.1600-051X.2006.01014.x.

Abstract

Aim: Tissue formation at the implant interface is known to be sensitive to mechanical stimuli. The aim of the study was to compare the bone formation around immediately loaded *versus* unloaded implants in two different implant macro-designs.

Material and Methods: A repeated sampling bone chamber with a central implant was installed in the tibia of 10 rabbits. Highly controlled loading experiments were designed for a cylindrical (CL) and screw-shaped (SL) implant, while the unloaded screw-shaped (SU) implant served as a control. An *F*-statistic model with $\alpha = 5\%$ determined statistical significance.

Results: A significantly higher bone area fraction was observed for SL compared with SU ($p < 0.0001$). The mineralized bone fraction was the highest for SL and significantly different from SU ($p < 0.0001$). The chance that osteoid- and bone-to-implant contact occurred was the highest for SL and significantly different from SU ($p < 0.0001$), but not from CL. When bone-to-implant contact was observed, a loading (SL *versus* SU: $p = 0.0049$) as well as an implant geometry effect (SL *versus* CL: $p = 0.01$) was found, in favour of the SL condition.

Conclusions: Well-controlled immediate implant loading accelerates tissue mineralization at the interface. Adequate bone stimulation via mechanical coupling may account for the larger bone response around the screw-type implant compared with the cylindrical implant.

Key words: animal; bone chamber; immediate loading; implant macro-design; peri-implant healing

Accepted for publication 24 September 2006

The light microscopical direct bone-to-implant contact is the final goal of implant healing and the first requirement for the long-term success of endosseous dental implants (Brånemark et al. 1977). The mechanisms underlying the peri-implant healing process are very similar to those occurring during bone fracture repair and involve the stages of haematoma, clot resolution and osteogenic cell migration, leading to the formation of new bone at the wound site (Davies & Hosseini 2000). These tissue responses depend on several factors among which implant material and design, implant surface characteristics, anatomical site and mechanical conditions are the most relevant. Bone formation adjacent to endosseous implants with various design and surface characteristics and at different anatomical locations has extensively been studied in undisturbed healing conditions, i.e. without loading, in animal experiments (Akimoto et al. 1999, Berglundh et al. 2003, Botticelli et al. 2003a, b, 2004, Franchi et al. 2004, 2005, Rimondini et al. 2005). Many aspects of early wound healing around endosseous implants have been elucidated (Slaets et al. 2006) and reviewed by Raghavendra et al. (2005). It is suggested that treatment outcomes are critically dependent upon implant design and surface characteristics that optimize the biological responses of early endosseous peri-implant healing (Davies 2003). Szmukler-Moncler et al. (1998) summarized data from animal studies on the histological status of implants loaded during the healing period. Conflicting data were obtained and could in part be assigned to implant

Conflict of interest and source of funding statement

The authors declare that they have no conflict of interest. Lies Geris is a research assistant and Joke Duyck is a postdoctoral research fellow of the Fund for Scientific Research Flanders.
This study was supported by the Research Council of the Katholieke Universiteit Leuven (Belgium) (OT/02/50) and the Fund for Scientific Research Flanders (Belgium) (O6260).

design and loading protocol. Clinical and experimental trials investigating fracture healing provide evidence that limited and well-controlled movement of fracture fragments stimulates callus formation and increases its mechanical stability (Goodship 1992, Claes et al. 1998). Awareness of the initial mechanical conditions provides a firm basis for potential mechanical and biological approaches regarding the enhancement of fracture healing (Klein et al. 2003).

Despite the fact that loading of implants immediately after their placement involves certain biological risks, the use of immediately loaded dental implants has been introduced in clinical routine for the last decade. It is no longer believed that immediate loading per se leads to fibrous encapsulation of implants (Szmukler-Moncler et al. 2000). On the contrary, mechanical signals have a pronounced influence on the development and differentiation of mesenchymal cells (Carter 1987). A certain amount of microstrain can therefore even promote early peri-implant osteogenesis (Piattelli et al. 1993, Simmons et al. 1999, 2001, Meyer et al. 2004). However, only a few well-controlled experimental studies have investigated the effect of mechanical load on tissue differentiation at the tissue–implant interface in vivo. Control of micromotion at the bone–implant interface is probably one of the most significant biological requirements for a load-bearing implant. A recently developed bone chamber model (Duyck et al. 2004) allows the evaluation of the tissue response around implants under well-controlled mechanical conditions.

Also, the implant configuration is considered to have a significant influence on the development of the bone–implant interface. The initial mechanical stability (primary stability) obtained during the implant installation is gradually replaced by a biological fixation of the implant (secondary stability). This early peri-implant osteogenesis is not only dependent on the loading history but also on the implant macro-design. Therefore, it is crucial to design an implant that distributes functional forces at a desirable level of intraosseous strains. A screw implant design develops a greater ability to transfer forces (Skalak 1985, Bidez & Misch 1992) as well as a higher mechanical retention than e.g. a cylindrical implant. The screw design minimizes micromotion of the implant during function and thereby upholds the primary stability, which has been considered to be the principal requirement for immediate loading success (Hall et al. 2005). Additionally, the thread design increases the surface area, compared with a cylinder (Misch 1999). Hence, it is generally recommended in the clinic to use threaded-type implants (Batenburg et al. 1998, Karoussis et al. 2004), in particular for immediate loading. It is also important to note that favourable clinical outcome with cylinder-type implants has been documented when a delayed loading regime was used (Wheeler 1996, Meijer et al. 2004a, b). However, the cylinder-type implant would appear contraindicated for immediate or early loading regimes due to lowering of primary stability and less resistance to vertical movement and shear stress (Watzak et al. 2005).

The aim of this study was to investigate the bone formation around immediately loaded implants *versus* the unloaded control and to study the influence of the implant macro-design. It was hypothesized that immediate loading of implants accelerates tissue mineralization at the interface depending on the implant configuration.

Material and Methods

Bone chamber model, loading device and implants

Duyck et al. (2004) developed a model to study the bone formation adjacent to endosseous implants under very well-controlled mechanical conditions. This model has successfully been used to conduct loading experiments (Duyck et al. 2006). Dual-structure perforated hollow TiAl6V4 cylinders were designed with a centrally positioned c.p. titanium implant. The hollow cylinders, called outer and inner bone chamber, fit exactly into each other and have corresponding perforations, allowing blood inflow and tissue growth into the central cavity of the cylinders. The central implant that is stabilized in a gliding bearing counting for the primary stability can be loaded in a well-defined and well-controlled manner by means of an external loading device or actuator (Fig. 1). This actuator consists of a piezo translator (pre-loaded closed loop LVPZT translator, P-841.60, ALT, Best, the Netherlands), which can induce a displacement of up to 90 μm and a load cell (XFTC 100-M5M-1000N, FGP Sensors, Les Clayes sous Bois Cedex, France) with a capacity of 1000 N in tension and 100 N in compression. A closed loop control assures the required displacement, thereby inducing shear stresses and strains in the tissue surrounding the implant. The load can be applied with a frequency of up to 50 Hz. The actuator is controlled by software written in ''Test Point''. Variations in load parameters such as displacement, forces, frequency, duration and amount and distribution of load cycles are possible. The applied forces and displacements are visualized on the computer screen during the load application and saved to a file. The actuator can easily be mounted onto the outer hollow cylinder and be connected to the implant. Immobilization of the animal during the loading session is ensured so that additional movement of the animal does not interfere with the implant loading.

In the current experiment, a cylindrical turned *versus* a screw-type turned implant of c.p. titanium (grade 2) was designed (Fig. 2) and decontaminated by soaking in a 4% HF–20% HNO_3 solution for 60 s, resulting in an R_a-value of 0.70 μm for both designs.

Surgical procedure

Ten 6-month-old female New Zealand white rabbits with an average weight of 4.064 kg (range: 3.590–4.250 kg) were included in the experiments. All rabbits were specific pathogen free (*Pasteurella* bacteria) and kept in quarantaine for $1\frac{1}{2}$ months before the study was started. To install the outer bone chamber, the animals were pre-medicated with an intramuscular neuroleptic analgesic (Vexylan® 1 mg/kg body weight, CEVA, Brussels, Belgium) and with an intramuscular anaesthetic (Ketamine 1000® 15 mg/kg, CEVA) and anaesthetized with propofol intravenously (Diprivan® 1%, 0.4 ml/kg body weight/hour, AstraZeneca, Brussels, Belgium). A circular incision was made on the medial side of the proximal tibia and the skin was released from the periosteum. A cavity was made centrally on the metaphysis and further manually widened by use of consecutively larger burrs. When a diameter of 10 mm was obtained, the outer bone chamber was installed press-fit, containing a Teflon cylinder to prevent tissue growth into the outer bone chamber during the osseointegration. Skin adherence to the periosteum by suturing at a distance of the bone chamber was performed to ensure skin stabiliza-

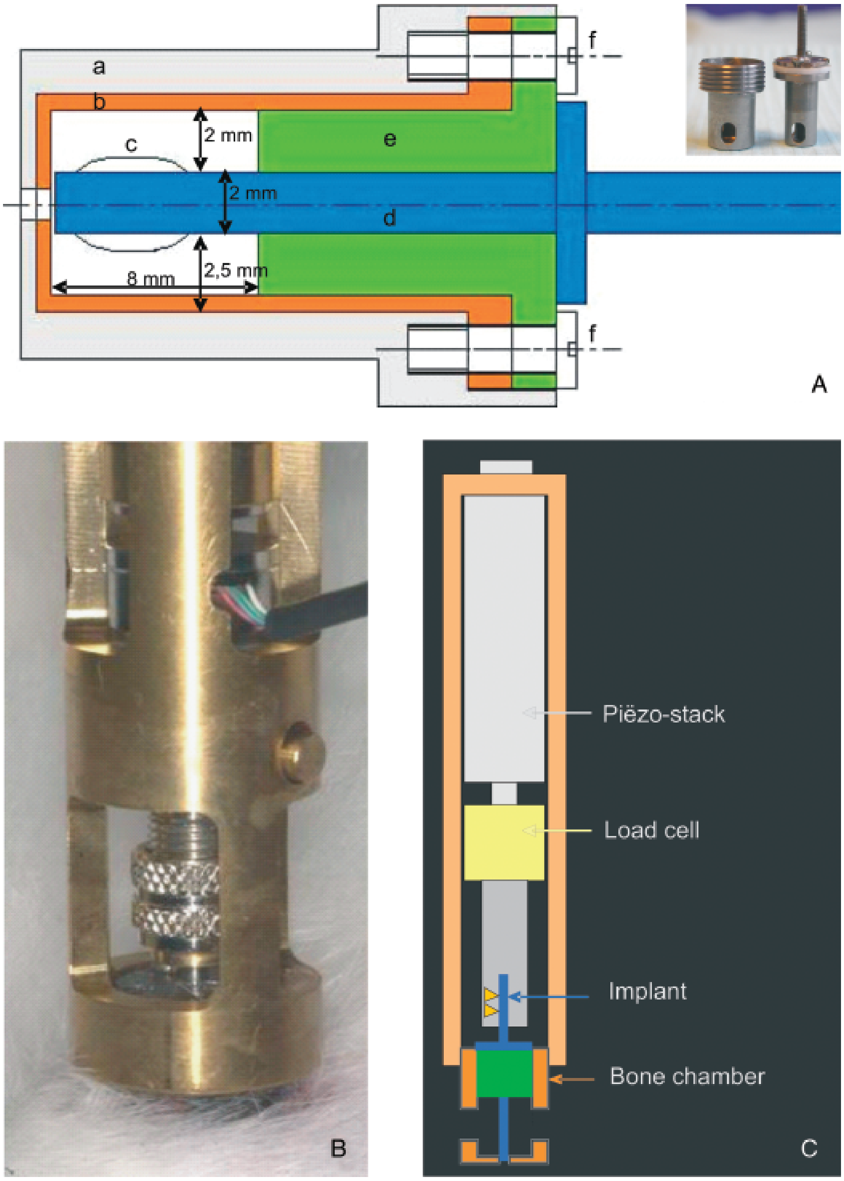

Fig. 1. (A) Schematic drawing of the experimental bone chamber. (a) outer bone chamber, (b) inner bone chamber, (c) perforations, (d) central implant, (e) Teflon bearing, (f) connecting screws (See, Duyck et al. 2004). (B) Custom made loading device screw-retained onto the outer bone chamber *in situ*. (C) Schematic drawing of the loading device.

tion. To prevent any micro-motion at the bone–bone chamber interface, the rabbit's leg was splinted with an elastic adhesive bandage (Tensoplast, BSN Medical, Leuven, Belgium) for 3–4 weeks. Post-operatively, the animals were given intramuscular bupreforfin as an analgenic (Temgesic® 0.05 mg/kg body weight, Schering-Plough NV, Brussels, Belgium) and antibiotics (penicilline) were administered intramuscularly 5 days post-operatively at a dose of 300,000 E/d daily (Kela NV, Hoogstraten, Belgium).

Twelve weeks following the outer bone chamber installation, the inner bone chamber and the central implant were installed. During this surgical procedure, the rabbits were only sedated with the combination of the agents listed above (ketamine and xylazine) and no anaesthesia was needed. The interior of the outer bone chamber was cleaned with physiological serum and prophylactic antibiotics (polymixine powder) were applied. Blood flow through the perforations into the lumen of the bone chamber was ensured by curetting the bone at the perforations. A new experiment was started as soon as the new inner bone chamber was put in place. At the end of the study, the animals were sacrificed with a 0.1 ml/kg bodyweight intravenous injection of a embutramide-mebenzoniumjodide-tetracaïne HCl solution (T61®, Intervet, Mechelen, Belgium).

The study protocol was approved by the regional ethics committee for laboratory animal research of the K.U.Leuven and was performed according to the Belgian animal welfare regulations and guidelines.

Loading protocols

Highly controlled loading experiments were designed for a cylindrical (CL) and screw-shaped (SL) c.p. titanium implant. Four hundred loading cycles of 30 μm implant displacement at a frequency of 1 Hz were applied three times a week during a period of 9 weeks. The unloaded condition for the screw design (SU) served as control (Table 1). Owing to its re-usability, the same bone chamber was used for all three experiments and test and control could be evaluated within the same animals. The different loading conditions were randomized in time as well as in sequence.

Specimen preparation and analyses

To evaluate the tissue growth into the bone chamber lumen and the bone response around the implant, the specimens were prepared for histological analysis. After harvesting the inner bone chamber content, the tissue blocks with implant were fixed in a $CaCO_3$-buffered formalin solution and dehydrated in an ascending series of ethanol concentrations over 18 days. Embedding was performed by infiltration of a benzoylperoxide (0.018%)–methylmetacrylate solution over 7 days. Sectioning transversely perpendicular to the implant and grinding were performed using a diamond saw. Five sections at the level of the perforations for each harvested bone chamber were reduced to a final thickness of 20 to 30 μm by micro-grinding and polishing using a cutting-grinding device. The sections were stained with a combination of Stevenel's blue and Von Gieson's picrofuchsin, visualizing mineralized bone tissue (red) and non-mineralized tissue (grey–green) (Fig. 3).

Histological examinations were performed under a light microscope at a magnification of × 40, × 100 and × 400. The assessments of the histomorphometrical proportions were performed on a computer screen (magnification $\times$ 100) by means of a high-sensitivity colour video camera (JVC TK-1280E,

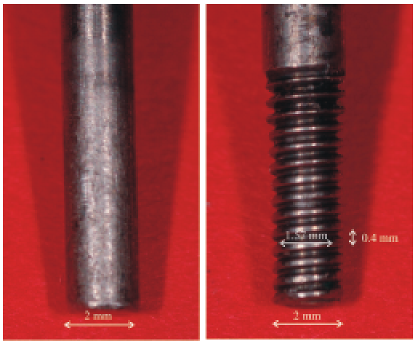

Fig. 2. Cylindrical (left) and screw-shaped (right) c.p. titanium implant (grade 2) (R_a-value 0.70 μm).

JVC Ibaraki-ken, Japan) mounted on the light microscope (Leitz Laborlux S, Wetzlar, Germany) and by means of a semiautomatic procedure (Image Pro Plus®, Media Cybernetics, Silver Spring, MD, USA). Data were pooled into a software program (Microsoft Excel®), and relative values were calculated for each histological section:

- Tissue area fraction (TAF, %): the percentage area of the inner bone chamber occupied by tissue.
- Bone area fraction (BAF, %): the whole spongy bone area (bone trabeculae and bone marrow) expressed as a percentage of the tissue area.
- Non-mineralized bone fraction (nMB, %): the percentage of the bone area occupied by non-mineralized bone trabeculae.
- Mineralized bone fraction (MB, %): the percentage of the bone area occupied by mineralized bone trabeculae.
- Osteoid-to-implant contact (OIC, %): the fraction of non-mineralized bone in direct contact with the implant surface.
- Bone-to-implant contact (BIC, %): the fraction of mineralized bone in direct contact with the implant surface.
- Bone-and-osteoid-to-implant contact (BOIC, %): the fraction of mineralized and non-mineralized bone in direct contact with the implant surface.

Table 1. Loading parameters for a cylindrical and screw-shaped c.p. titanium implant positioned in the same bone chamber installed in the tibia of mature New Zealand white rabbits ($n = 10$)

	Implant macro-design	Duration of the experiment (weeks)	Number of loading sessions/ week	Displacement (μm)	Frequency (Hz)	Number of cycles/ loading session
Experiment 1	Cylinder	9	3	30	1	400
Experiment 2	Screw	9	3	30	1	400
Experiment 3	Screw	9	–	–	–	–

The origin of the sections was blinded during histological and histomorphometrical analyses. Illustrations of the histomorphometrical measurements are shown in Fig. 4.

Statistical analysis

A linear mixed model was used with the experimental animal as a random effect and the loading condition (Exp 1 →

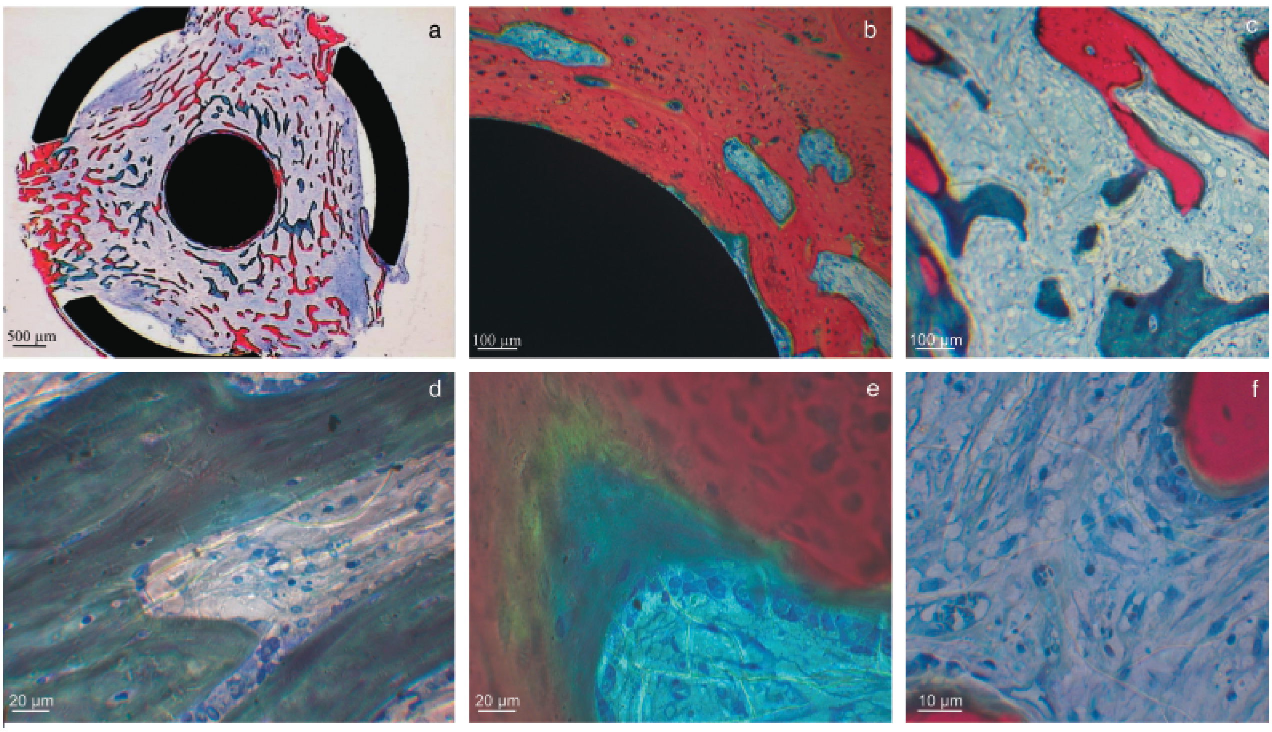

Fig. 3. (a) Representative histological section of an inner bone chamber harvested 9 weeks after installation; (b) illustrates bone-and-osteoid-to-implant contact; (c) mineralized (red) and non-mineralized (green/grey) bone trabeculae can be easily distinguished; (d) (e) trabeculae lined with osteoblasts; osteocytes found within the newly formed bone tissue; (f) well organized bone marrow lying in between the trabeculae. Stevenel's blue and Von Gieson's picrofuchsin stain.

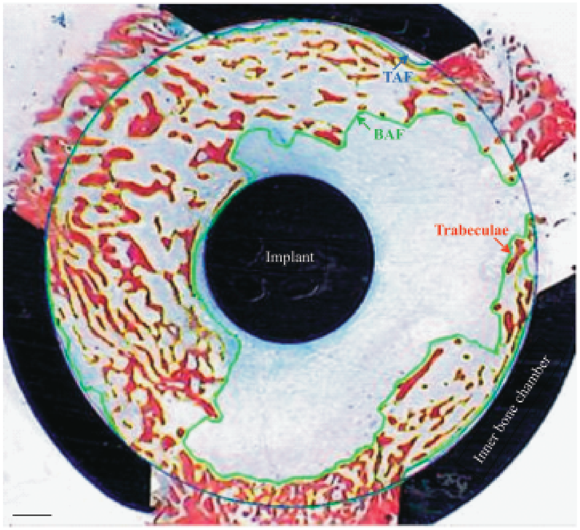

Fig. 4. Illustration of histomorphometric measurements. Tissue area fraction (TAF), % area of the bone chamber occupied by tissue; Bone area fraction (BAF), the whole spongy bone area expressed as % of the tissue area; Non-mineralized/mineralized bone fraction (nMB/MB), % of the bone area occupied by non-mineralized/mineralized bone trabeculae. Stevenel's blue and Von Gieson's picrofuchsin stain; Bar = 500 μm.

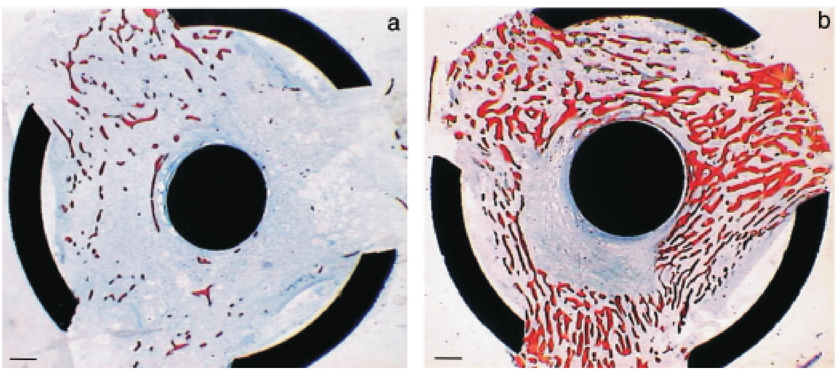

Fig. 5. Few and thin bone trabeculae for the unloaded (SU) condition (a) and numerous and thick trabeculae crossing the marrow spaces for the loaded (CL) condition (b). Stevenel's blue and Von Gieson's picrofuchsin stain; Bar = 500 μm.

Exp 3), number of histological section (1 → 5) and harvest number (1 → 3) as fixed effects for the histomorphometric parameters TAF, BAF, nMB and MB. Owing to the absence of bone contact with the implant in several samples, logistic transformation of the data was performed for the parameters BIC, OIC and BOIC. A logistic mixed model, calculating the chance that bone-and/or-osteoid-to-implant contact occurred and a proportional odds mixed model, taking into account the amount of bone-and/or-osteoid-to-implant contact, were used. A linear mixed model was also used on the subset of data where implant contact was observed.

The data were analysed with SAS/STAT statistical software (SAS Institute Inc., Cary, NC, USA). An *F*-statistic model with an α-level of 0.05 was chosen to determine the statistical significance. Post hoc multiple comparisons were performed using the Bonferroni's method for significant *F*-tests.

Results

All outer bone chambers healed well and threefold sampling of the inner bone chamber was performed successfully. Loading of the implant took place uneventfully at all times and was well accepted by the animals, without the need for sedation or anaesthesia.

Gross histological observations

Signs of infection were observed in 9.3% of the histological sections. The latter were excluded from data analysis because of interaction risk on the tissue formation inside the bone chamber.

After 9 weeks, most of the bone chamber was filled with newly formed tissue and comprised of a mixture of bone trabeculae, bone marrow and connective tissue. The bone trabeculae appeared to originate from the pre-existing bone outside the bone chamber. The bone marrow was well organized and contained large numbers of adipocytes and blood vessels. The trabeculae were lined with osteoblasts and osteocytes were found within the newly formed bone tissue. Besides mineralized bone, non-mineralized osteoid tissue was also observed on most histological sections (Fig. 3). The tissue inside the bone chamber after 9 weeks of undisturbed healing (SU condition) was dominated by adipocytes and loose connective tissue. Few and mostly thin trabeculae of mineralized bone were present. Loaded implants (conditions CL and SL) showed more numerous newly formed bone trabeculae crossing interstitial spaces (Fig. 5). The latter histological tissue architecture was similar for both loaded conditions.

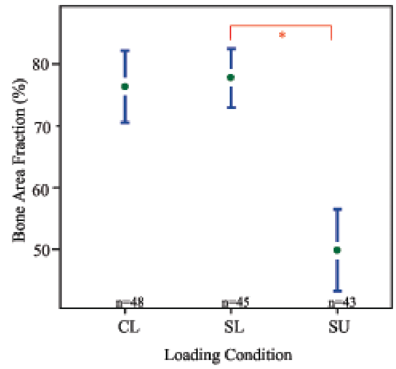

Fig. 6. Mean values ± SD/$\sqrt{n}$ of the bone area fraction for the variable Loading Condition. Significant differences ($p < 0.0033$) are indicated with *. (n = number of observations)

Morphometric assessments

Interaction was found between the fixed effect loading condition and the other fixed effects (number of the histological section and harvest number) for the parameter TAF. Therefore, the effect of the loading condition could not be assessed independently.

The results of the morphometric measurements BAF, nMB and MB for the fixed effect loading condition are presented in Figs 6 and 7. Significantly less

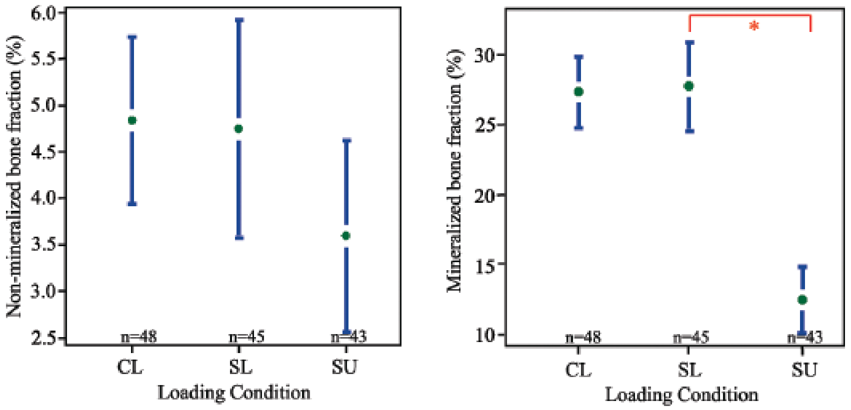

Fig. 7. Mean values ± SD/$\sqrt{n}$ of the non-mineralized bone fraction (left) and mineralized bone fraction (right) for the variable Loading Condition. Significant differences ($p<0.01$) are indicated with *. (n = number of observations)

BAF was observed in the screw-unloaded (SU) condition compared with the loaded (SL) condition ($p<0.0001$). The cylinder-loaded (CL) and screw-loaded (SL) situations resulted in similar BAF mean values. Neither loading nor implant geometry effect was found for nMB. MB was the highest for the SL condition and was statistically significant with the SU condition ($p<0.0001$).

Bone-and-osteoid-to-implant contact occurred in 42.65% of the histological sections. The results for OIC, BIC and BOIC are shown in Fig. 8. Statistically significant differences are shown for the logistic mixed and proportional odds mixed model analysis (red) and for the linear mixed model analysis (green). Owing to the absence of contact in more than half of the sections, the percentages of OIC, BIC and BOIC are higher than those shown in the figure. The logistic mixed model as well as the proportional odds statistical analysis, both using the whole dataset, revealed that the chance that OIC, BIC and BOIC occurred was the highest under the SL condition and significantly different from the SU condition ($p<0.0001$). No implant geometry effect was found. When the linear mixed model was applied on the subset of data where implant contact was observed, no differences were found between the three different conditions for OIC. On the contrary, a loading effect ($p=0.0049$) as well as an implant geometry effect ($p=0.01$) was found for BIC, with the highest mean values obtained for the SL condition. The influence of the implant design was no longer significant for the composed BOIC variable ($p=0.0456$) while the loading effect remained ($p=0.0006$), with the highest mean values obtained for the SL condition.

The position of the histological section relative to the bottom of the bone chamber had a significant effect on the histomorphometric measurements BAF, BIC and BOIC. Values were generally higher for the sections closest to the bottom of the bone chamber.

The effect of the harvest number was significant for all parameters, except for BIC. BAF, nMB, OIC and BOIC were the highest in the last performed experiment, while MB was the highest for the second experiment.

Discussion

The experimental model used in the present study allowed the study of bone formation around implants with various configurations and under well-controlled mechanical conditions. The formation of bone is a multi-step process that is characterized by interactions between various cells, components of the extracellular matrix and inorganic materials. It is known that mechanical injury is able to stimulate cells with bone-forming capacity to multiply and form bone (Carter et al. 1998). The findings demonstrated that indeed hard tissue formation occurred in the bone chamber, similar to hard tissue formation in tooth extraction and fracture sites. New bone was observed to have formed in the bone chamber, despite the wide initial gap between the bone and the implant surface of 2 mm. The composition of the new tissue formed inside the bone chamber was clearly dependent on the mechanical conditions. Moreover, at the implant surface, a different tissue response was observed depending on the implant design.

The major portion of the bone chamber was filled after 9 weeks with calcified tissue. Bone formation appeared to extend from the bone at the perforations up to the implant positioned in the centre of the bone chamber. This pattern of bone formation is consistent with what has been coined distance osteogenesis (Osborn & Newesely 1980). When comparing the tissue composition after 9 weeks of unloaded or loaded healing, it was noted that the tissue in the bone chamber was dominated by bone marrow (mainly occupied by adipocytes) for the unloaded implants, while the tissue around loaded implants was dominated by many bone trabeculae. Similar observations were reported in an experiment evaluating the bone tissue formation in tooth extraction sites (Cardaropoli et al. 2003). The authors investigated the bone-healing dynamics and observed that between 5 and 12 weeks, most of the bone formed within the extraction socket had been replaced with bone marrow. They suggested that the extraction socket was exposed to minimal load and hence, there was apparently no obvious demand for mineralized tissue (trabecular bone) in the compartment. In some respect, the observations of the current experimental model are in agreement with these findings and a similar small mineralized bone/bone marrow ratio was observed for the unloaded condition. However, this ratio was extensively higher for the loaded condition and a spongy trabecular network was observed in the bone chamber in this case.

The effect of applied loading on bone tissue formation was evident in this model, with loaded bone chambers having increased BAF and MB relative to the unloaded controls. The loading parameters were selected in an attempt to correlate the micromovements in the bone chamber to the mechanosensitivity of bone cells on the one hand and to the loading conditions of oral implants on the other. In former studies with the bone chamber (Duyck et al. 2006, Vandamme et al. 2006), a 30 µm implant displacement was found to influence significantly the tissue differentiation and bone formation around cylindrical implants. A number of loading cycles of 400 at a frequency of 1 Hz was expected to have a good cellular response (Kaspar

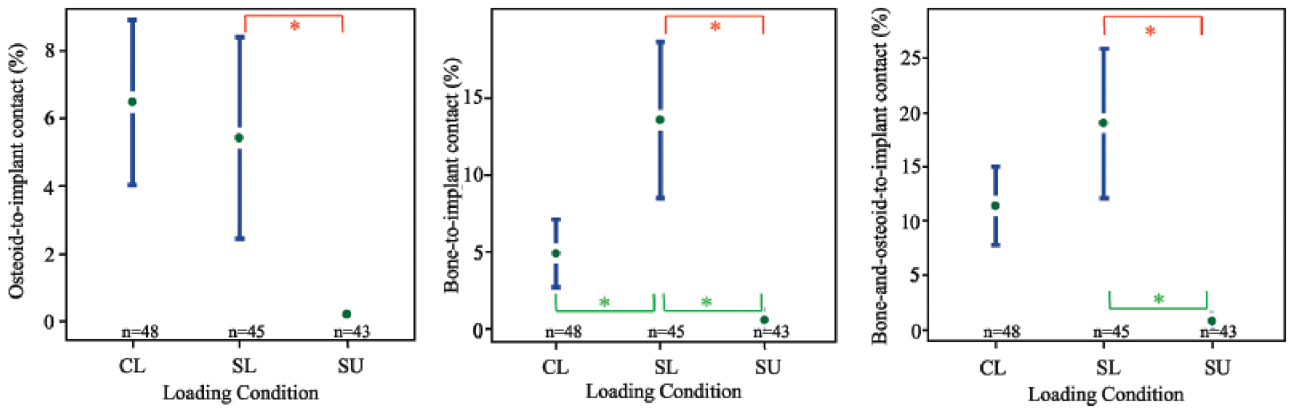

Fig. 8. Mean values ± SD/$\sqrt{n}$ of the osteoid-to-implant contact (left), bone-to-implant contact (middle) and bone-and-osteoid-to-implant contact (right) for the variable Loading Condition. Significant differences for the logistic mixed model and the proportional odds mixed model ($p < 0.0033$) are shown with * in red and for the linear mixed model ($p < 0.01$) in green. (n = number of observations)

et al. 2002). The number of cycles mimics the known daily tooth contact time during biting and swallowing in humans (Graf 1969). The loading frequency corresponds to the chewing frequency (1–2 Hz) in humans. Experiments lasting for 9 weeks allowed a higher incidence of hard tissue implant contact compared with 6-weeks experiments (Duyck et al. 2006, Vandamme et al. 2006), while tissue regeneration under the influence of mechanical stimulation was still ongoing. In this way, it was assumed that the loading protocol of the current study appropriately stimulated the tissues surrounding the implant. A significant difference was found between the SL and SU conditions for BAF and MB, with much higher mean values obtained for the SL condition (Figs 6 and 7). These results indicate that mechanical loading had a positive effect on the bone formation in the bone chamber. A well-controlled mechanical stimulus onto the implant was secured by the protected environment of the bone chamber and therefore potentially interfering factors could be excluded. Similar results were reported by van der Meulen et al. (2006), who studied the effects of mechanical loading applied in vivo to native cancellous bone in the rabbit on bone formation and trabecular realignment. They developed a novel device allowing well-defined in vivo loading of the native cancellous bone in the rabbit's tibia and demonstrated that mechanical loading increased bone formation and altered trabecular morphology, with significantly greater trabecular thickness in loaded condyles compared with the contralateral unloaded limb.

Similar values for nMB were found for all three test conditions, suggesting that the process and rate of bone formation in the bone chamber is uniform. No influence of the implant geometry could be established for all these variables, suggesting that at a certain distance of the interface, tissues are formed and remodelled independently of the implant design. To confirm this hypothesis, the tissue composition should be quantified and compared for areas of interest of different size, circular around the implant. Finite-element analysis could additionally describe the stress distribution pattern not only at the interface but also further away in the bone chamber. Such studies are underway.

Bone-to-implant contact was observed in 35.29% of the tissue samples and OIC in 32.35%. Implant contact was predominantly found under the loaded conditions while only 2.21% BIC and 1.47% OIC could be attributed to the SU condition (Fig. 8 – red accolades). These histomorphometric observations indicate that the mechanical conditions under the CL and SL conditions favoured the establishment of osseointegration. The strains at the interface, induced by the implant micromotion, exerted a positive effect on osseointegration. In this particular case, the 30 μm displacement of the implant seemed to fall within the limits of tolerated micromotion for both the cylindrical and screw-type implant design. A similar finding for cylindrical implants was established in a previous study with the bone chamber (Vandamme et al. 2006), where a 30–50 μm micromotion was found to stimulate the bone formation at the implant surface compared with an unloaded situation. In the present study, the effect of a 30 μm immediate displacement was investigated for both the cylindrical and screw-type configuration. It was hypothesized that the implant design converted this displacement into a distinct mechanical stimulus, as suggested by Pilliar et al. (1995), leading to a different tissue response at the interface. When analysing the subset of data where implant contact was present, it was found that the loaded screw-type implant exhibited significantly more BIC than the loaded cylindrical implant (Fig. 8 – green accolades). This implant geometry effect was no longer found for the composed variable BOIC due to a high mean value for OIC at the CL interface. Similar to the results of nMB, no loading effect could be established for OIC. These results confirm that the implant design indeed has an effect on the tissue response at the loaded interface most likely due to a distinct biomechanical coupling. The mineralization of the tissues surrounding the screw-type implant was enhanced by loading the implant, while the interface of a cylindrical implant was characterized by more non-mineralized tissue that is less prone to mechanical loading.

On the histological sections where no implant contact was present, a different composition and organization of the tissue in the vicinity of the implant surface could be observed, depending on the loading history. A well-organized dense connective tissue with cells and collagen fibres, running parallel to the implant surface, was observed for loaded implants while enlarged marrow spaces (fatty and fibrous) were found near the surface of the unloaded implants. The tissue micro-architecture in the area adjacent to the implant seemed to reflect the mechanical micro-environment. These findings are in line with the results of Neugebauer et al. (2006), who studied the peri-implant bone organization after 4 months of undisturbed healing and under an immediate loading regimen in minipigs. They reported a different collagen fibres orientation for both groups as well as a different tissue composition adjacent to the implant. Loaded implants displayed a higher quantity of secondary osteons, whereas unloaded implants were surrounded by a higher quantity of marrow spaces. Similarly, for the histological sections with absence of implant contact, we were able to attribute a specific tissue organization to the loading condition but not to the implant design. The zone of circular collagen fibers around the loaded implants is indicative of healing by fibrous encapsulation, whereas poorly differentiated and less organized tissue with high amounts of marrow spaces adjacent to the unloaded implant might further differentiate under the influence of loading.

The number of harvests was examined as a fixed effect in the statistical analyses to investigate whether a bone fatigue effect exists for the bone chamber model. The results indicated that such an effect does not exist. No exhaustion effect for bone growth in a bone chamber has been reported by other authors as well (Goodman et al. 1993, Duyck et al. 2006). On the contrary, higher mean values for the several parameters were recorded for the second and the last performed experiment compared with the first one.

Promising results have been observed when endosseous wound healing under load is allowed (Attard & Zarb 2005). Besides surgery-, host- and load-related factors, implant-related factors may also influence the outcome of immediate implant loading (Gapski et al. 2003). Adequate force transfer between an implant and the surrounding tissues is essential. Bone stimulation via biomechanical coupling may account for the positive effect of micromovements on the establishment of osseointegration. However, these micro-movements at the bone–implant interface are tolerated up to a certain threshold and is design and/or surface state dependent (Szmukler-Moncler et al. 1998). A numerical in vitro investigation analysing the stress distribution in the surrounding bone for different implant designs by means of a finite element method showed that different implant shapes lead to variations in stress distribution (Siegele & Soltesz 1989). Tada et al. (2003) reported in a finite-element analysis a better biomechanical environment for implants placed in high-density trabecular bone. In low-density bone, screw-type implants exhibit a lower maximum equivalent strain under axial load than cylinder-type implants. In a similar bone chamber study (Duyck et al. 2006), attempting to define the tolerated micro-motion threshold, even a 30 μm micromovement already impaired osseointegration. The substantial difference from this study, however, was that their use of turned cylindrical implants did not allow an efficient force transfer to the surrounding tissues. This underlines the importance of a good biomechanical coupling in the establishment of osseointegration.

This experimental set-up differs from the clinical situation in which implants are installed in healed extraction sites where the implant is, at least in some areas, in direct contact with the host bone. Likewise, the experiment mimics more the immediate tooth replacement clinical situation where, mostly at the apex, the implant is in direct contact with the host bone, whereas more coronally only a blood cloth surrounds the implant. Primary mechanical implant stability was obtained through the device itself through the central gliding bearing and was only interrupted during the loading sessions. The bone chamber offers a good methodology to search for optimization of healing and osseointegration of implants surrounded by an initial gap under the influence of loading. This model presents a most arduous endeavour to obtain osseointegration, and therefore an interesting one to study tissue differentiation in the implant surroundings and early peri-implant osteogenesis under the influence of controlled loading.

The metaphysis of the rabbit tibia was chosen to install the bone chamber. This cancellous site consists of a small amount of trabecular bone and a considerable amount of bone marrow, rich in undifferentiated cells and blood vasculature, surrounded by compact bone. The selected anatomical location allowed blood flow into the bone chamber and colonization with mesenchymal cells. Differentiation of these cells with bone-forming capacities resulted in trabecular bone formation in the bone chamber that was found to be dependent on the mechanical situation. The rabbit's tibia has optimal anatomical dimensions, is easy to access and mimics the mandibular situation, both having thick cortical plates. However, extrapolation of the findings of this study to the human situation should be performed with caution. It is not the observations as such but rather the differences between the observations of the test conditions that need to be emphasized.

Given the challenges inherent in in vivo well-controlled immediate loading experiments of implants, the findings of the present study are promising and demonstrate the sensitivity of bone formation to the mechanical conditions at the peri-implant site. A 30 μm implant displacement enhanced bone formation in the implant surroundings. Additionally, the screw-shaped implant design promoted osseointegration by providing a favourable local mechanical environment for bone formation compared with the cylindrical implant. In the clinic, screw-shaped implants not only favour primary stability, but might improve the so-called secondary stability achieved by physiological loading.

Acknowledgements

The authors would like to acknowledge the expert help of Prof. B. Van Damme of the Department of Morphology and Molecular Pathology of the Katholieke Universiteit Leuven. The authors are indebted to Michel De Cooman of the Department of Electrical Engineering – ESAT-MICAS of the Katholieke Universiteit Leuven for the technical support.

References

Akimoto, K., Becker, W., Persson, R., Baker, D. A., Rohrer, M. D. & O'Neal, R. B. (1999) Evaluation of titanium implants placed into simulated extraction sockets: a study in dogs. *International Journal of Oral and Maxillofacial Implants* **14**, 351–360.

Attard, N. J. & Zarb, G. A. (2005) Immediate and early implant loading protocols: a literature review of clinical studies. *Journal of Prosthetic Dentistry* **94**, 242–258.

Batenburg, R. H., Meijer, H. J., Raghoebar, G. M., Van Oort, R. P. & Boering, G. (1998) Mandibular overdentures supported by two Brånemark, IMZ or ITI implants. A prospective comparative preliminary study: one-year results. *Clinical Oral Implants Research* **9**, 374–383.

Berglundh, T., Abrahamsson, I., Lang, N. P. & Lindhe, J. (2003) De novo alveolar bone formation adjacent to endosseous implants. *Clinical Oral Implants Research* **14**, 251–262.

Bidez, M. W. & Misch, C. E. (1992) Force transfer in implant dentistry: basic concepts and principles. *Journal of Oral Implantology* **18**, 264–274.

Botticelli, D., Berglundh, T., Buser, D. & Lindhe, J. (2003a) Appositional bone formation in marginal defects at implants. *Clinical Oral Implants Research* **14**, 1–9.

Botticelli, D., Berglundh, T., Buser, D. & Lindhe, J. (2003b) The jumping distance revisited: an experimental study in the dog. *Clinical Oral Implants Research* **14**, 35–42.

Botticelli, D., Berglundh, T. & Lindhe, J. (2004) Hard-tissue alterations following immediate implant placement in extraction sites. *Journal of Clinical Periodontology* **31**, 820–828.

Brånemark, P. I., Hansson, B. O., Adell, R., Breine, U., Lindstrøm, J., Hallen, O. & Ohman, A. (1977) Osseointegrated implants in the treatment of the edentulous jaw. Experience from a 10-year period. *Scandinavian Journal of Plastic and Reconstructive Surgery* **16** (Suppl.), 1–132.

Cardaropoli, G., Araujo, M. & Lindhe, J. (2003) Dynamics of bone tissue formation in tooth extraction sites. An experimental study in dogs. *Journal of Clinical Periodontology* **30**, 809–818.

Carter, D. R. (1987) Mechanical loading history and skeletal biology. *Journal of Biomechanics* **20**, 1095–1109.

Carter, D. R., Beaupré, G. S., Giori, N. J. & Helms, J. (1998) Mechanobiology of skeletal regeneration. *Clinical Orthopaedics and Related Research* **1**, 41S–55S.

Claes, L. E., Heigele, C. A., Neidlinger-Wilke, C., Kaspar, D., Seidl, W., Margevicius, K. J. & Augat, P. (1998) Effects of mechanical factors on the fracture healing process. *Clinical Orthopaedics and Related Research* **355** (Suppl.), S132–47.

Davies, J. E. (2003) Understanding peri-implant endosseous healing. *Journal of Dental Education* **67**, 932–949.

Davies, J. E. & Hosseini, M. M. (2000) Histodynamics of endosseous wound healing. In: Davies, J. E. (ed). *Bone Engineering*, pp. 1–14. Toronto: Em Squared Inc.

Duyck, J., De Cooman, M., Puers, R., Van Oosterwyck, H., Vander Sloten, J. & Naert, I. (2004) A repeated sampling bone chamber methodology for the evaluation of tissue differentiation and bone adaptation around titanium implants under controlled mechanical conditions. *Journal of Biomechanics* **37**, 1819–1822.

Duyck, J., Vandamme, K., Geris, L., Van Oosterwyck, H., De Cooman, M., Vander Sloten, J., Puers, R. & Naert, I. (2006) The influence of micro-motion on the tissue differentiation around immediately loaded cylindrical turned titanium implants. *Archives of Oral Biology* **51**, 1–9.

Franchi, M., Fini, M., Martini, D., Orsini, E., Leonardi, L., Ruggeri, A., Giavaresi, G. & Ottani, V. (2005) Biological fixation of endosseous implants. *Micron* **36**, 665–671.

Franchi, M., Orsini, E., Trire, A., Quaranta, M., Martini, D., Piccari, G. G., Ruggeri, A. & Ottani, V. (2004) Osteogenesis and morphology of the peri-implant bone facing dental implants. *The Scientific World Journal* **14**, 1083–1095.

Gapski, R., Wang, H. L., Mascarenhas, P. & Lang, N. P. (2003) Critical review of immediate implant loading. *Clinical Oral Implants Research* **14**, 515–527.

Goodman, S., Wang, J. S., Doshi, A. & Aspenberg, P. (1993) Difference in bone ingrowth after one versus two daily episodes of micromotion: experiments with titanium chambers in rabbits. *Journal of Biomedical Materials Research* **27**, 1419–1424.

Goodship, A. E. (1992) Mechanical stimulus to bone. *Annals of the Rheumatic Diseases* **51**, 4–6.

Graf, H. (1969) Bruxism. *Dental Clinics of North America* **13**, 659–665.

Hall, J., Miranda-Burgos, P. & Sennerby, L. (2005) Stimulation of directed bone growth at oxidized titanium implants by macroscopic grooves: an in vivo study. *Clinical Implant Dentistry and Related Research* **7**, S76–82.

Karoussis, I. K., Bragger, U., Salvi, G. E., Burgin, W. & Lang, N. P. (2004) Effect of implant design on survival and success rates of titanium oral implants: a 10-year prospective cohort study of the ITI Dental Implant System. *Clinical Oral Implants Research* **15**, 8–17.

Kaspar, D., Seidl, W., Neidlinger-Wilke, C., Beck, A., Claes, L. & Ignatius, A. (2002) Proliferation of human-derived osteoblast-like cells depends on the cycle number and frequency of uniaxial strain. *Journal of Biomechanics* **35**, 873–880.

Klein, P., Schell, H., Streitparth, F., Heller, M., Kassi, J. P., Kandziora, F., Bragulla, H., Haas, N. P. & Duda, G. N. (2003) The initial phase of fracture healing is specifically sensitive to mechanical conditions. *Journal of Orthopaedic Research* **21**, 662–669.

Meijer, H. J., Batenburg, R. H., Raghoebar, G. M. & Vissink, A. (2004a) Mandibular overdentures supported by two Brånemark, IMZ or ITI implants: a 5-year prospective study. *Journal of Clinical Periodontology* **31**, 522–526.

Meijer, H. J., Raghoebar, G. M., Van 't Hof, M. A. & Visser, A. (2004b) A controlled clinical trial of implant-retained mandibular overdentures: 10 years' results of clinical aspects and aftercare of IMZ implants and Brånemark implants. *Clinical Oral Implants Research* **15**, 421–427.

Meyer, U., Joos, U., Mythili, J., Stamm, T., Hohoff, A., Fillies, T., Stratmann, U. & Wiesmann, H. P. (2004) Ultrastructural characterization of the implant/bone interface of immediately loaded dental implants. *Biomaterials* **25**, 1959–1967.

Misch, C. E. (1999) Implant design considerations for the posterior regions of the mouth. *Implant Dentistry* **8**, 376–386.

van der Meulen, M. C., Morgan, T. G., Yang, X., Baldini, T. H., Myers, E. R., Wright, T. M. & Bostrom, M. P. (2006) Cancellous bone adaptation to in vivo loading in a rabbit model. *Bone* **38**, 871–877.

Neugebauer, J., Traini, T., Thams, U., Piattelli, A. & Zoller, J. E. (2006) Peri-implant bone organization under immediate loading state. Circularly polarized light analyses: a minipig study. *Journal of Periodontology* **77**, 152–160.

Osborn, J. F. & Newesely, H. (1980) Dynamic aspects of the implant-bone interface. In: Heimke, G. (ed). *Dental Implants: Materials and Systems*, pp. 111–123. München: Carl Hanser Verlag.

Piattelli, A., Ruggeri, A., Franchi, M., Romasco, N. & Trisi, P (1993) A histologic and histomorphometric study of bone reactions to unloaded and loaded non-submerged single implants in monkeys: a pilot study. *The Journal of Oral Implantology* **19**, 314–320.

Pilliar, R. M., Deporter, D. & Watson, P. A. (1995) Tissue-implant interface: micromovements effects. In: Vincenzini, P. (ed). *Materials in Clinical Applications, Advances in Science and Technology*. Faenza: Techna: 569–579.

Raghavendra, S., Wood, M. C. & Taylor, T. D. (2005) Early wound healing around endosseous implants: a review of the literature. *The International Journal of Oral and Maxillofacial Implants* **20**, 425–431.

Rimondini, L., Bruschi, G. B., Scipioni, A., Carrassi, A., Nicoli-Aldini, N., Giavaresi, G., Fini, M., Mortellaro, C. & Giardino, R. (2005) Tissue healing in implants immediately placed into postextraction sockets: a pilot study in a mini-pig model. *Oral Surgery, Oral Medicine, Oral Pathology, Oral Radiology and Endodontics* **100**, e43–50.

Siegele, D. & Soltesz, U. (1989) Numerical investigations of the influence of implant shape on stress distribution in the jaw bone. *The International Journal of Oral & Maxillofacial Implants* **4**, 333–340.

Simmons, C. A., Meguid, S. A. & Pilliar, R. M. (2001) Mechanical regulation of localized and appositional bone formation around bone-interfacing implants. *Journal of Biomedical Materials Research* **55**, 63–71.

Simmons, C. A., Valiquette, N. & Pilliar, R. M. (1999) Osseointegration of sintered porous-surfaced and plasma spray-coated implants: an animal model study of early postimplantation healing response and mechanical stability. *Journal of Biomedical Materials Research* **47**, 127–138.

Skalak, R. (1985) Aspects of biomechanical considerations. In: Branemark, P. I., Zarb, G. & Albrektsson, T. (eds). *Tissue-Integrated Prosthesis: Osseointegration in Clinical Dentistry*, pp. 117–128. Chicago: Quintessence.

Slaets, E., Carmeliet, G., Naert, I. & Duyck, J. (2006) Early cellular responses in cortical bone healing around unloaded titanium implants: an animal study. *Journal of Periodontology* **77**, 1015–1024.

Szmukler-Moncler, S., Piattelli, A., Favero, G. A. & Dubruille, J. H. (2000) Considerations preliminary to the application of early and immediate loading protocols in dental implantology. *Clinical Oral Implants Research* **11**, 12–25.

Szmukler-Moncler, S., Salama, H., Reingewirtz, Y. & Dubruille, J. H. (1998) Timing of loading and effect of micromotion on bone-dental implant interface: review of experimental literature. *Journal of Biomedical Materials Research* **43**, 192–203.

Tada, S., Stegaroiu, R., Kitamura, E., Miyakawa, O. & Kusakari, H. (2003) Influence of implant design and bone quality on stress/strain distribution in bone around implants: a 3-dimensional finite element analysis. *The International Journal of Oral and Maxillofacial Implants* **18**, 357–368.

Vandamme, K., Naert, I., Geris, L., Vander Sloten, J., Puers, R. & Duyck, J. (2006) Histodynamics of bone tissue formation around immediately loaded cylindrical implants in the rabbit. A bone chamber model. *Clinical Oral Implants Research*, in press.

Watzak, G., Zechner, W., Ulm, C., Tangl, S., Tepper, G. & Watzek, G. (2005) Histologic and histomorphometric analysis of three types of dental implants following 18 months of occlusal loading: a preliminary study in baboons. *Clinical Oral Implants Research* **16**, 408–416.

Wheeler, S. L. (1996) Eight-year clinical retrospective study of titanium plasma-sprayed and hydroxyapatite-coated cylinder implants. *International Journal of Oral and Maxillofacial Implants* **11**, 340–350.

Address:
Prof. J. Duyck
Department of Prosthetic Dentistry/BIOMAT Research Group
School of Dentistry
Oral Pathology and Maxillofacial Surgery
Faculty of Medicine
Katholieke Universiteit Leuven (K.U.Leuven)
Kapucijnenvoer 7
B-3000 Leuven
Belgium
E-mail: Joke.Duyck@uz.kuleuven.be

Clinical Relevance

Scientific rationale for the study: Bone healing under physiological loading is becoming a common clinical practice, although conflicting data from experimental studies emphasize the importance of the loading protocol and implant design when immediate loading is applied.

Principal findings: The positive effect of controlled immediate loading on bone formation around implants was demonstrated. In addition to the primary mechanical stability inherent in a screw-shaped implant, its secondary biological stability is most likely improved by a more favourable mechanical coupling for bone formation compared with the cylindrical implant.

Practical implications: It becomes evident that well-controlled immediate loading accelerates peri-implant tissue mineralization. In the clinic, osseointegration of implants can be accelerated by immediate loading unless careful selection of the loading protocol in relation to the bone characteristics and the implant design is carried out.